

# Intelligent Integration of Active BMS and Multilevel Converter: A Unique Topology and Experimental Validation for Enhanced AC Battery System Control

İrfan Güven Çömezoğlu<sup>\*,1</sup>, Erol Çıracı<sup>1</sup>, Dilara Bayar<sup>2</sup>, Alim Kerem Erdoğan<sup>2</sup>, Ali Kafalı<sup>2</sup>

\*guven@inorobotics.com.tr, ORCID: 0000-0002-6951-0995

<sup>1</sup>R&D, Inovasyon Mühendislik, Eskişehir, Türkiye

<sup>2</sup>R&D, ACD Veri Mühendisliği, Eskişehir, Türkiye

**Abstract:** In this study, a modular AC battery system based on a multilevel converter (MLC) that eliminates the need for a conventional DC–AC inverter is presented. In the proposed architecture, each battery module contains both the energy storage element and a two-switch power stage, and a stepped AC voltage can be generated directly through series-connected modules. In this way, compared to conventional two-level inverter solutions, the number of components, system volume, and weight are reduced, while power conversion efficiency is increased. In addition, with the active Battery Management System (BMS) integrated into each battery module, low-loss active balancing is performed at both cell and module levels, aiming to reduce cell imbalances, increase usable capacity, and extend battery lifetime. The developed system is first modeled in MATLAB/Simulink and analyzed through simulations, and then experimentally validated on a hardware-in-the-loop (HIL) test setup and a low-power laboratory prototype. The obtained results show that an efficiency above 95% and a total harmonic distortion (THD) below 3% are achieved at approximately 5 kW power level. The study demonstrates that the MLC-based AC battery approach with integrated active BMS offers a high-efficiency and compact alternative for both mobile and stationary energy storage applications.

**Keywords:** Battery management system, Battery energy storage systems, Multilevel converter, Hardware-in-the-loop, Active balancing.

## INTRODUCTION

DC–AC power conversion in electric vehicles (EVs) and energy storage systems is generally carried out using conventional inverters. However, the use of inverters adds an additional stage to the energy conversion chain, reducing overall system efficiency and introducing drawbacks in terms of cost, weight, and volume. Particularly in mobile applications, the inverter and the required cooling components occupy significant space in vehicles and increase the total weight. As a solution to these problems, a new approach that eliminates the need for an inverter is required.

In this study, an AC battery system is proposed that offers an innovative solution to this issue. The proposed system features a multilevel converter (MLC)-based topology that switches the battery modules so as to generate the AC voltage directly. By appropriately switching the battery modules, the system can produce the desired AC output without the need for a DC–AC inverter. With this approach, the number of power conversion stages is reduced, energy efficiency is increased, and the physical dimensions and weight of the system are significantly decreased. Unlike existing MLC applications, in the developed topology only two

semiconductor switching devices are used in each battery module, enabling a highly simple and optimized circuit design. This simple design not only reduces the complexity of the control circuitry but also decreases switching losses and overall system cost.

The study also incorporates the integration of an active Battery Management System (BMS) that provides active balancing in battery management. In conventional passive BMS systems, voltage differences between cells are dissipated through resistors and converted into heat, leading to energy waste. In contrast, active balancing transfers excess energy from one cell to another, thereby minimizing energy losses and ensuring that each cell remains within a safe voltage range. The integrated active BMS aims to extend battery lifetime by ensuring balanced utilization of the cells.

The proposed AC battery system is modeled in the MATLAB/Simulink environment and simulations are carried out. In addition, a hardware prototype is implemented in the laboratory, and real-time validation is obtained through Hardware-in-the-Loop (HIL) tests. Experimental studies show that the proposed system achieves high efficiency (>95%), low harmonic distortion, and fast dynamic response. The findings indicate that the MLC-based AC battery concept, which completely eliminates the need for an inverter, provides significant benefits in terms of both energy efficiency and system simplification. In this respect, the study represents an important step towards increasing the commercial feasibility of MLC-based AC battery systems.

## STATE OF THE ART AND LITERATURE REVIEW

In electric vehicles and grid-scale energy storage systems, studies aiming at more integrated and efficient designs of power converter and battery units have been rapidly increasing. In this context, AC battery structures integrated with Modular Multilevel Converters (MLC) attract significant attention. Thanks to the multilevel structure of the MLC architecture, a high-quality output waveform, low harmonic distortion, and increased fault tolerance can be achieved, while also providing the capability of monitoring and control at the battery cell level [1,2]. The AC battery concept, on the other hand, increases efficiency and reduces the need for additional converter stages by arranging the battery to generate AC voltage directly, thereby combining the functions of the inverter and the battery [3,4]. Studies have shown that this approach offers a more modular, scalable, and highly efficient solution compared to conventional two-level inverters [2,5].

Active cell balancing techniques increase the usable capacity in battery packs by equalizing SoC and voltage differences without energy loss and reduce performance degradation caused by imbalance [6]. The integration of these methods into MLC-based AC battery systems enables the unification of both power conversion and balancing operations within a single structure and reduces the need for additional BMS hardware [7,8]. In particular, the positive impact of active balancing on battery lifetime in high-power applications is emphasized in the literature [9].

From a thermal management perspective, the presence of power electronic components and cells within the same structure increases heat density; therefore, cooling design is of great importance. Air-cooled systems are widely preferred, especially in automotive applications, due to their low cost and lightweight advantages, and can provide sufficient performance with proper duct design and heat sinks [9,10]. Research in the literature shows that safe operating temperatures can be maintained in AC battery systems with well-designed air-cooling solutions [1].

Overall, it is observed that MLC-based AC battery architectures constitute a strong alternative for both electric vehicles and stationary storage systems due to their high efficiency, flexible control, integrated active balancing, and simplified power electronics structures [11-13].

## SYSTEM ARCHITECTURE AND CIRCUIT DESIGN

### A. General Architecture of the Proposed AC Battery System

The proposed AC battery system is built on a multilevel converter (MLC) architecture consisting of modular battery units connected in series. Each module includes a battery group with a certain DC voltage level and a two-switch power stage integrated into this group. By connecting the modules in series, the total DC voltage level is formed; as a result of driving the modules with appropriate switching strategies, a stepped AC output is generated directly from the series connection nodes.

### B. MLC Module Structure and Operating Principle

Each MLC module comprises a 12 V battery submodule, a half-bridge power stage with two MOSFETs, a gate driver, a local control and monitoring microcontroller, and internal measurement and protection circuits. In the proposed topology, multilevel voltage generation is achieved with only two switching devices per module: the MOSFETs are driven by complementary PWM signals so that one is on while the other is off, making the module output alternate between the battery voltage and 0 V depending on the instantaneous switching state.

The detailed circuit topology of the first module is given in Fig. 1. The circuit structures of the other modules are designed according to the same principle, except for the battery submodule voltage levels.

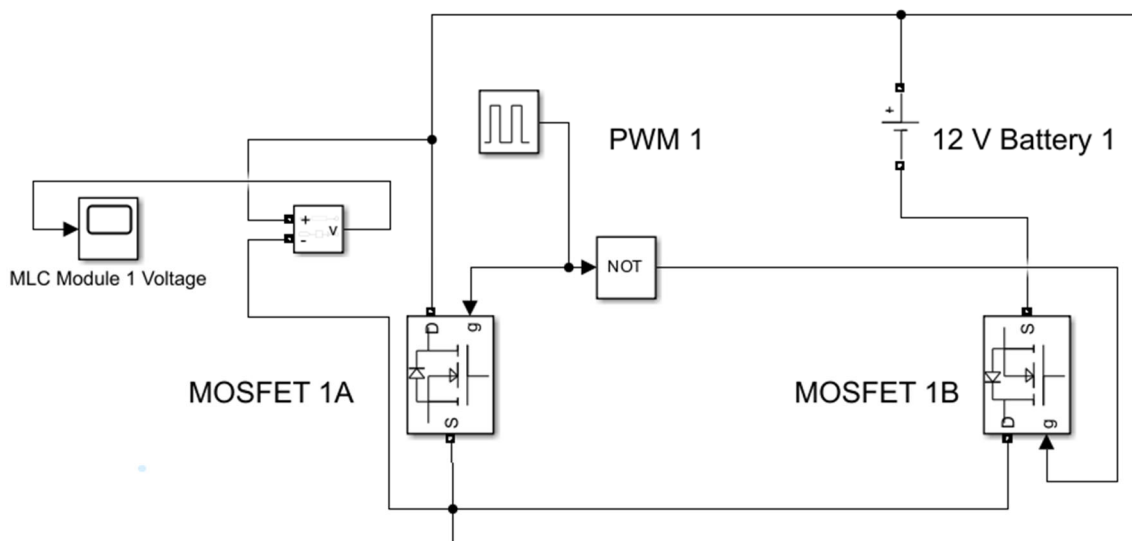


**Fig. 1.** MLC Module 1 Circuit

## BMS–MLC INTEGRATION AND ACTIVE BALANCING

In the proposed AC battery system, each MLC module acts both as a power converter and as a local battery management unit. To this end, an active BMS structure performing cell voltage and temperature measurement as well as active balancing is integrated into every module (see Fig. 2), so that balancing, which is conventionally handled by a separate external BMS, is fully embedded into the modular power stage [1,2,7]. This architecture enables state-of-charge (SoC) balancing both at cell level and between modules: for example, the participation of low-SoC modules in AC generation can be limited by the control algorithm, or energy transfer from other modules can be prioritized to increase the overall usable capacity of the system, in line with battery-integrated MLC concepts reported in the literature.

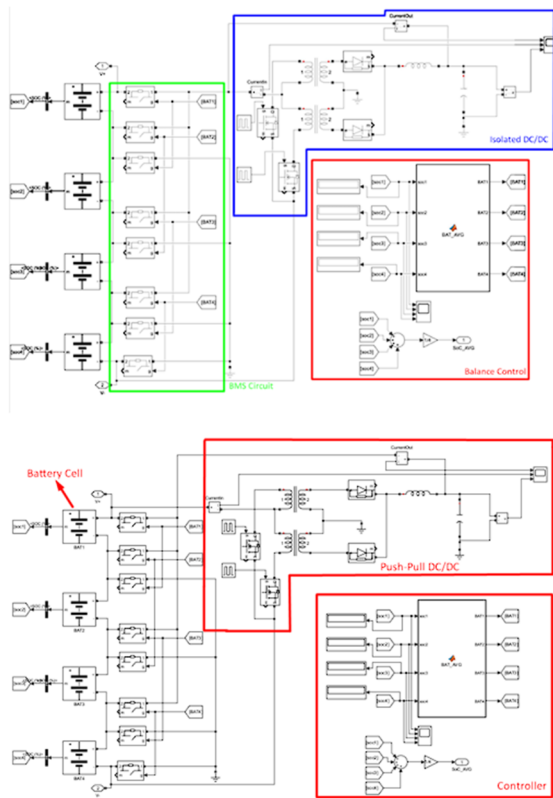


Fig. 2. Unique Circuit – Active balancing circuit

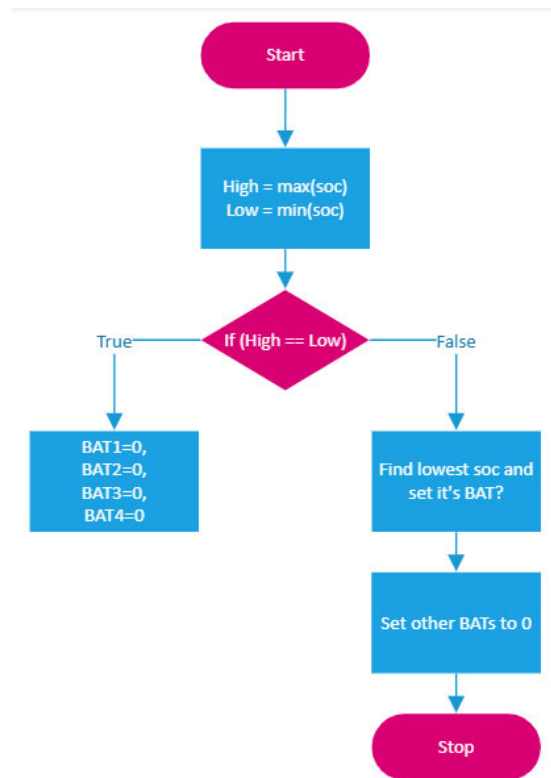


Fig. 3. Active balancing function flowchart

Owing to the inherent advantages of the multilevel converter architecture, harmonic components in the output voltage are reduced and operation at lower  $dV/dt$  levels becomes possible [5,13]. This decreases filter requirements and conversion losses, leading to higher efficiency. Measurements on the prototype show an efficiency above 95%, which is consistent with the 3–5% efficiency gains reported in previous studies [12]. The resulting efficiency improvement directly mitigates thermal stress on the cells and thus contributes to extended battery lifetime [9]. Moreover, literature reports that active balancing can increase the effective pack capacity by approximately 2% through improved SoC distribution [6].

The decision steps of the balancing algorithm used in the simulations are summarized in Fig. 3. In each cycle, the cell with the lowest SoC is prioritized for energy transfer, which minimizes unnecessary power circulation, shortens the overall balancing time, and limits additional losses.

## SIMULATION WORKS

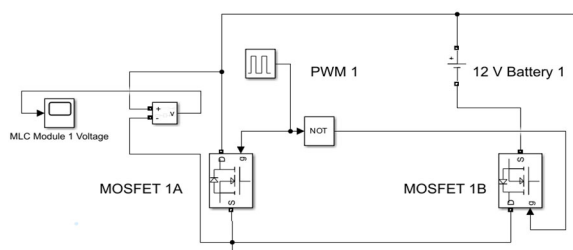
### A. Simulation Model and Parameters

The behavior of the proposed AC battery system was modeled and analyzed in detail in MATLAB/Simulink using four MLC modules representing  $\sim 12$  V battery submodules, each with a two-switch half-bridge power stage, whose outputs are connected in series to a single-phase line with a common resistive load, a commutator circuit for full-wave AC generation, an LC output filter to improve the sinusoidal waveform, and internal measurement blocks for voltage and current at both module and system level. The main simulation parameters are: grid/output fundamental frequency 50 Hz, module PWM switching frequency 10–20 kHz, nominal DC module voltage 12 V, four series-connected modules, and a single-phase resistive load scalable to approximately 5 kW, consistent with the laboratory prototype.

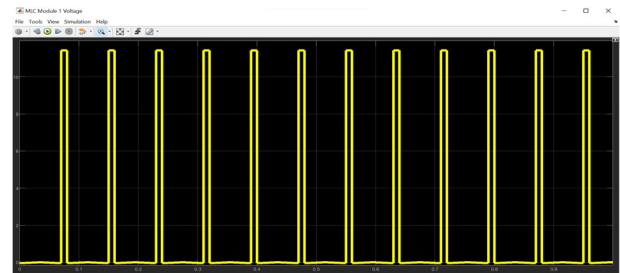
### B. Analysis of MLC Module and System-level Waveforms

Simulation results were first examined at the individual MLC module level. Fig. 4(a)–(h)

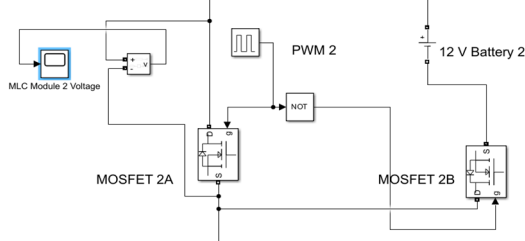
shows the circuit structures of the four modules and the corresponding output voltage waveforms obtained under complementary PWM operation. The stepped transition between the battery voltage and 0 V at each module output constitutes the basic multilevel structure.



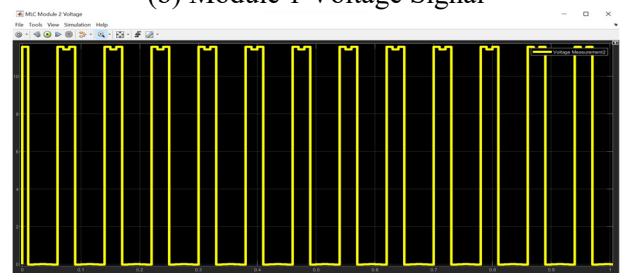
(a) Module 1 Circuit



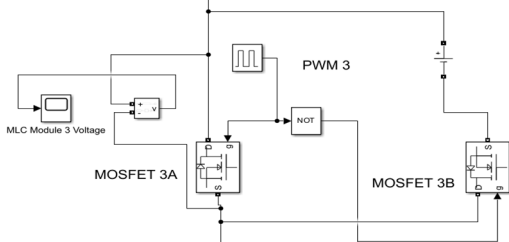
(b) Module 1 Voltage Signal



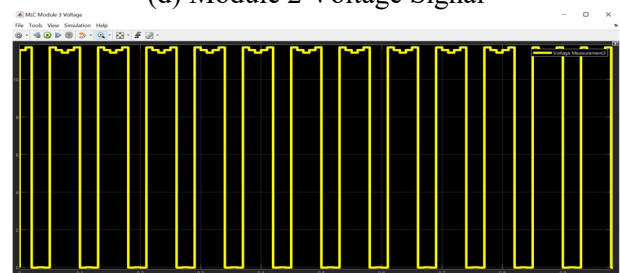
(c) Module 2 Circuit



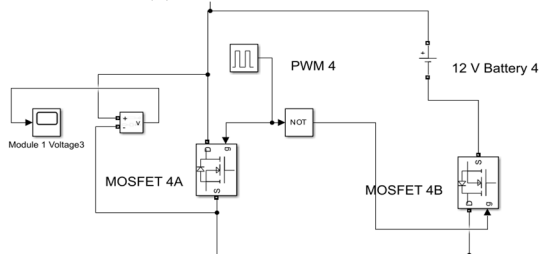
(d) Module 2 Voltage Signal



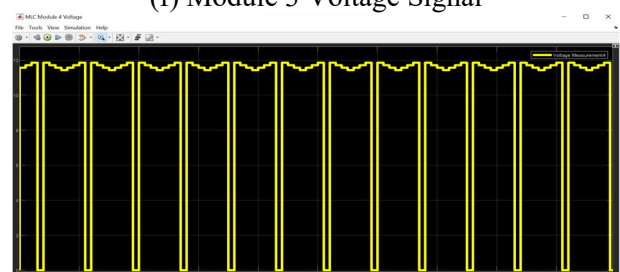
(e) Module 3 Circuit



(f) Module 3 Voltage Signal



(g) Module 4 Circuit



(h) Module 4 Voltage Signal

**Fig. 4.** Circuit structures and voltage output waveforms of the MLC modules

In the full system configuration where the module outputs are connected in series, the overall circuit structure of the four-module arrangement is given in Fig. 5. The resulting system-level output voltage and current waveforms, obtained from virtual sensors in the simulation model, are presented in Fig. 6 and Fig. 7.

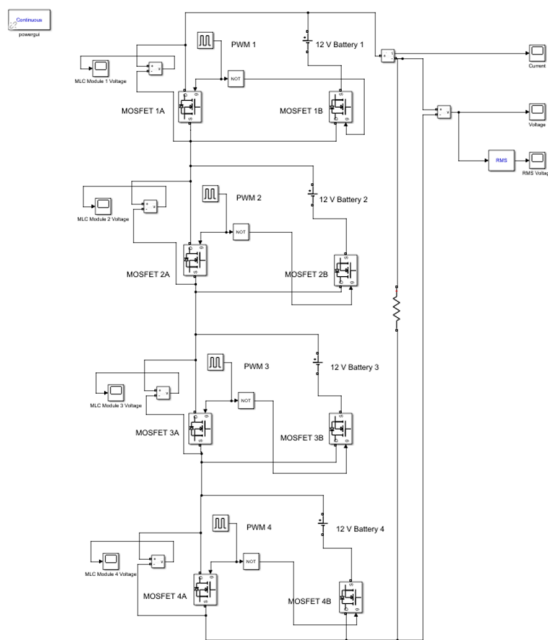


**Fig. 5.** Circuit Structure Combining Four Modules

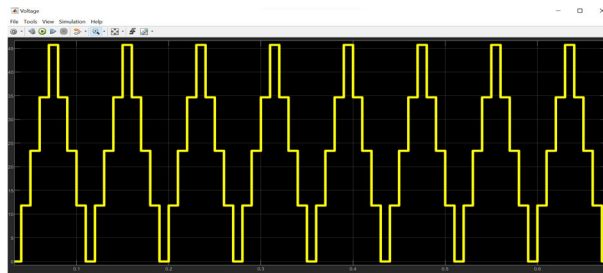


**Fig. 6.** Voltage Output When Four MLC Module Circuits Are Operating Simultaneously



**Fig. 7.** Current Output When Four MLC Module Circuits Are Operating Simultaneously

Despite the limited number of modules, the four-module configuration already produces a multilevel waveform whose fundamental component is close to a sinusoid. As the number of modules increases, the number of levels grows and the waveform approaches an ideal sine wave. The comparison of the obtained voltage and current waveforms with ideal sinusoidal references, shown in Fig. 8 and Fig. 9, confirms that the multilevel structure significantly reduces harmonic content compared to conventional two-level converters and, with an additional filter, can meet grid power quality standards.

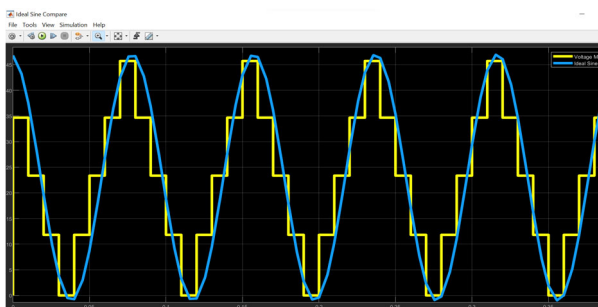


**Fig. 8.** Comparison of the voltage output obtained when four MLC Module circuits operate simultaneously with the ideal sinusoidal output

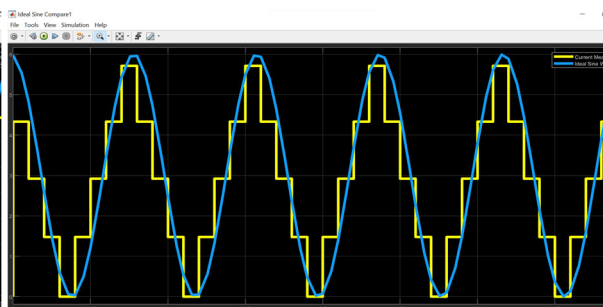


**Fig. 9.** Comparison of the current output obtained when four MLC Module circuits operate simultaneously with the ideal sinusoidal output

### C. Commutator and LC Filter Effects – Simulation Analysis

In the basic MLC structure, the modules can generate only positive output voltage, so a commutator circuit is added at the output to obtain a full-wave AC waveform. The schematic of the MLC with commutator is shown in Fig. 10, and the standalone commutator circuit in Fig. 11.

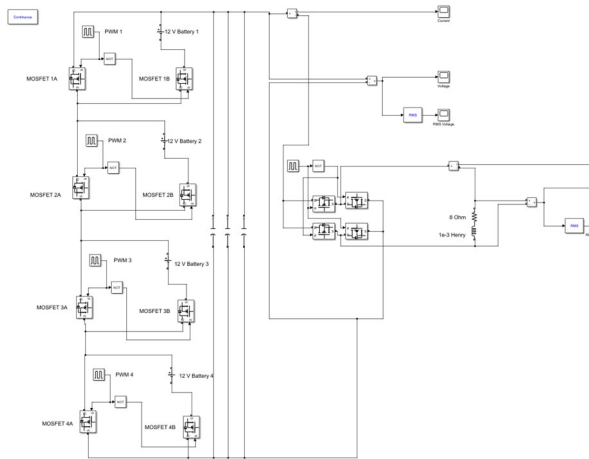


Fig. 10. MLC circuit with commutator

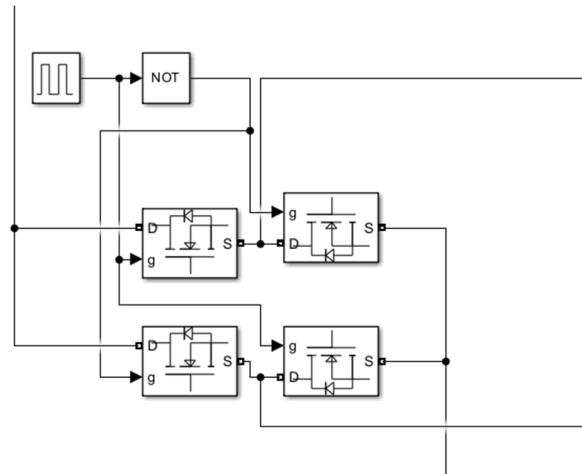


Fig. 11. Commutator circuit

When the commutator is activated, the positive voltage produced by the modules is applied to the load with alternating polarity according to the switching sequence, resulting in a full-wave AC output. The corresponding simulated output voltage and current waveforms are given in Fig. 12 and Fig. 13, respectively, confirming the generation of both positive and negative half cycles.

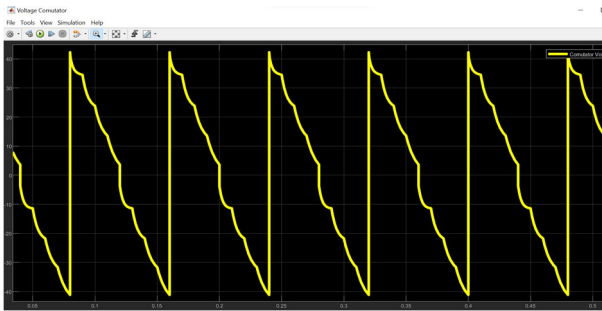


Fig. 12. Output voltage after adding the commutator

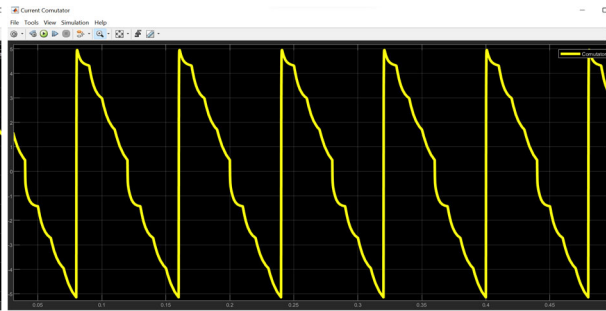


Fig. 13. Output current after adding the commutator

To further improve the sinusoidal character and suppress harmonics, an LC filter is connected to the output of the commutator-based structure. The updated single-module commutated MLC with LC filter is shown in Fig. 14.

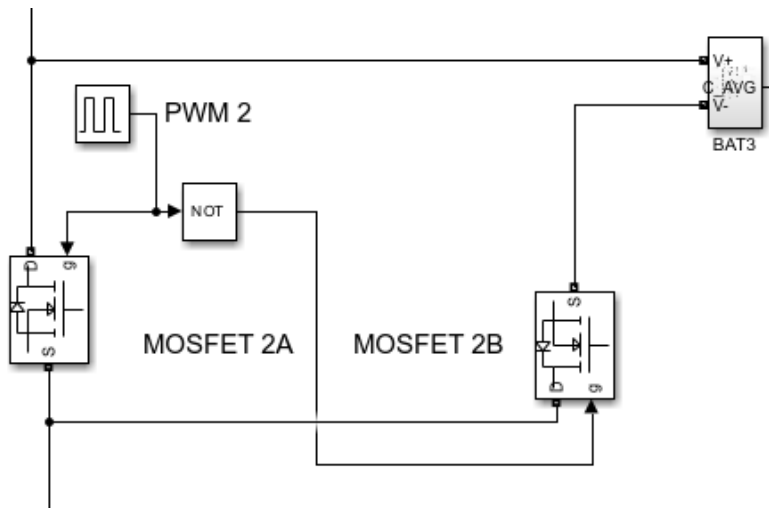


Fig. 14. Single MLC module with commutator and LC filter

The simulation results indicate that the LC filter significantly attenuates high-frequency harmonics without affecting the fundamental component and brings the output voltage and current waveforms very close to an ideal sinusoid. In combination with the multilevel topology, this allows grid-quality waveforms to be achieved with a relatively small number of modules.

#### *D. Loss and Efficiency Analysis – Theoretical Evaluation*

Although ideal switches and lossless conductors in simulation lead to an apparent efficiency close to 100%, conduction and switching losses must be considered in a practical design. Therefore, a theoretical efficiency estimation was carried out by combining the simulation results with MOSFET conduction and switching loss calculations. Conduction losses were obtained using the data-sheet on-state resistance and the simulated load current waveform, while switching losses were estimated from the data-sheet switching energies and the selected switching frequency.

A key advantage of the multilevel approach is that, for a given output quality, it can operate with a lower effective switching frequency and smaller voltage steps than a two-level inverter [2,5,12], directly reducing switching losses. In addition, the proposed topology uses only two switches per module, which lowers the total number of semiconductor devices compared to classical MMC submodules with eight switches [1,2], thereby decreasing both conduction and switching loss contributions.

Theoretical calculations show that, under nominal operating conditions, total semiconductor losses correspond to only a few percent of the output power, leading to a converter efficiency in the 95–98% range. These estimates are consistent with the experimental measurements reported in the Results section, where efficiencies above 96% were obtained with the laboratory prototype.

In summary, the simulations confirm that the proposed MLC-based AC battery architecture can generate a multilevel waveform, that the addition of the commutator and LC filter yields a near-sinusoidal full-wave output, and that system efficiency remains high even when realistic semiconductor losses are taken into account, in agreement with the subsequent HIL and hardware test results.

## PROTOTYPE DESIGN AND HARDWARE-IN-THE-LOOP (HIL) TESTS

### *A. Design of Prototype System Components*

The developed AC battery system was implemented as a laboratory-scale modular prototype to validate the simulation-based design. The prototype consists of battery modules integrating the MLC function and active BMS, a central master controller managing all modules, a power stage including load and measurement elements, and a real-time control/simulation unit interfaced with the HIL infrastructure.

Each battery module comprises a lithium-ion battery group of approximately 12 V, a half-bridge power stage with two MOSFETs connected to this battery, and a local microcontroller (STM32F4 series) responsible for control and monitoring. The modules are designed to be scalable to the desired voltage and current levels via series and parallel connection.

Inter-module communication is realized via a CAN bus: each module transmits measured cell voltages, temperatures, module current, and SoC to the central controller, while the master sends switching schedules and active balancing commands back over the same bus. The main components of the prototype system and their positions within the MLC HIL test platform are schematically illustrated in Fig. 15, and the physical layout of the demo setup is shown in Fig. 16.

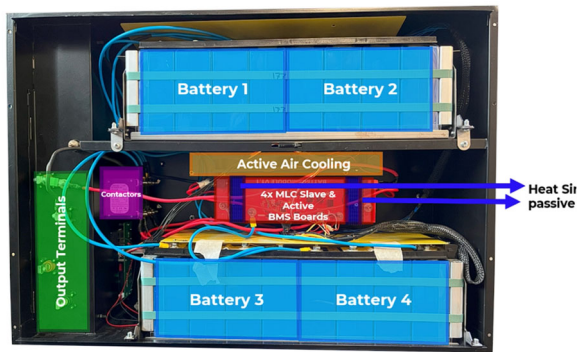


**Fig. 15.** HiL MLC system parts

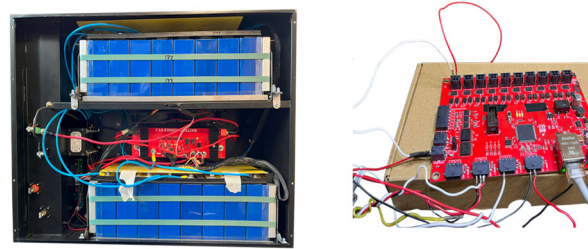


**Fig. 16.** Demo 1 environment parts

### B. Hardware and Software Integration

System control is handled by a central controller that synchronizes all modules. Using a single-phase 50 Hz AC reference, it determines the conduction intervals of each module and generates the corresponding PWM signals. Its main tasks are generating the AC reference waveform and module voltage references, producing complementary PWM signals for the two-switch MLC structure per module, maintaining inter-module phase and timing synchronization, and collecting measurement data via CAN while executing protection and shutdown actions in fault conditions. Local module controllers drive the MOSFETs according to central commands and manage the active balancing circuits based on cell-level measurements, yielding a distributed yet coordinated architecture for both power electronics control and battery management.

### C. HIL Test Environment and Procedures

A real-time Hardware-in-the-Loop (HIL) test setup was established to validate the prototype. A MATLAB/Simulink real-time model is interfaced bidirectionally with the physical MLC modules, enabling closed-loop testing. The HIL workflow comprises deployment of the model to the real-time platform, command transmission from the controller to the MLC modules, and acquisition of module feedback (voltage, current, temperature) for analysis. During tests, output waveforms, efficiency, harmonic content, and active balancing performance were recorded and compared with simulation results for validation. The overall demo layout and HIL platform structure are illustrated in the corresponding figures.

### D. Thermal Tests and Validation of the Cooling Arrangement

The thermal behavior of the prototype AC battery system was monitored with an infrared camera at different load levels during HIL tests. At light load, critical component temperatures remained close to ambient and spatially uniform (see Fig. 17). Under full-load conditions, the fan-assisted air-cooling scheme kept module temperatures below 40 °C, with heatsink placement and airflow paths shown in Fig. 18. These results confirm that the compact modular architecture operates within safe temperature limits without requiring additional liquid cooling.



Fig. 17. Thermal camera results under low load

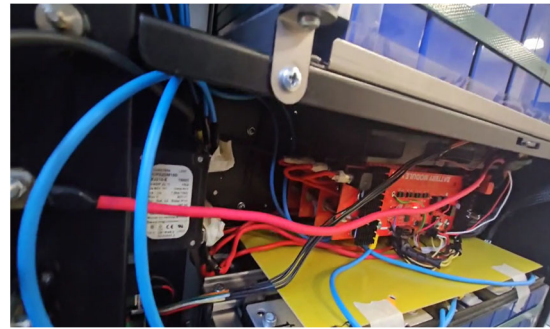


Fig. 18. Installation of heat sink cooling units on the MLC Slave card

E. Initial Tests: Power Quality and Efficiency Results

In the first validation stage, the power quality and efficiency of the prototype AC battery system were evaluated. Under an approximately 5 kW load, converter efficiency was measured above 96%, in good agreement with simulation results, and the output current THD was kept below 3% thanks to the commutator and LC filter. A typical AC output waveform is shown in Figure 20, and fast voltage regulation with stable dynamic behavior was observed during load transients.

F. Active-balancing BMS HIL Tests

The active balancing function was tested in real time within the HIL environment, where cell voltages and SoC values of each module were monitored via a dedicated interface (see Fig. 19). It was confirmed that balancing continues uninterrupted while AC power is being delivered; a representative HIL screenshot is given in Fig. 21. Intentionally introduced SoC mismatches were observed to decrease over time, as shown in Fig. 22, confirming that the active BMS operates successfully and consistent with simulation results.

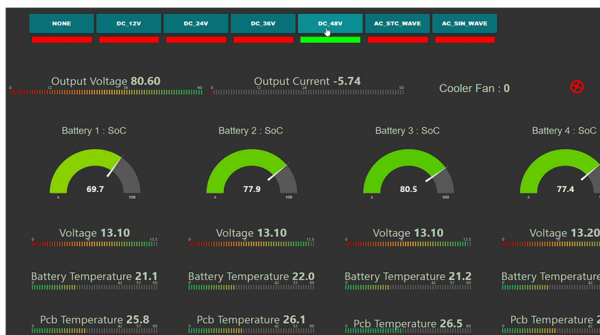


Fig. 19. Battery active balancing monitoring

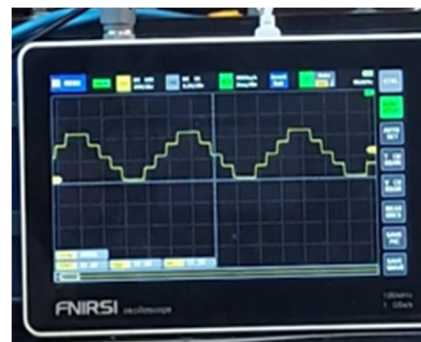


Fig. 20. MLC AC output waveform



Fig. 21. HIL environment during simultaneous

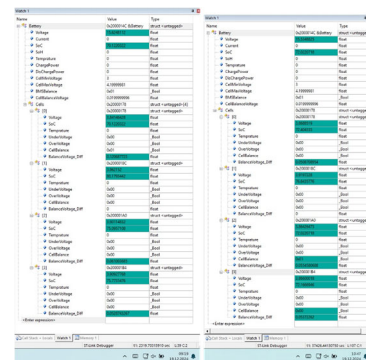


Fig. 22. Battery data and active balancing control screen

### *G. Improvement and Optimization Steps*

Following the initial HIL and prototype tests, several optimizations were implemented. The heatsink layout and airflow path were refined to reduce temperature gradients; PWM timing and inter-module load sharing were adjusted to improve dynamic response and current balancing; and lower-loss MOSFETs together with higher-accuracy sensors were adopted to enhance efficiency and control precision. As a result, the system's power quality, thermal performance, and efficiency reached the targeted levels, demonstrating scalability towards commercial applications.

## CONCLUSION

In this study, an MLC-based AC battery system capable of generating AC output without a separate inverter stage was developed, integrating an active-balancing BMS at the module level and validated through both simulations and experiments. Using only two switches per module reduces hardware complexity, while the multilevel voltage generation improves power quality and conversion efficiency.

Simulation and HIL-based prototype tests at around 5 kW demonstrated converter efficiencies above 95–96% and output current THD below 3% with the commutator and LC filter in place. The modular control strategy provided fast and stable response to load changes, and the active balancing function reduced SoC differences between modules over time, improving usable capacity in line with the ~2% gains reported in the literature.

Compared to commercial 48 V / 5 kW battery–inverter solutions, the proposed architecture offers higher efficiency, a more compact design, and the added benefit of integrated active balancing. Current limitations include the single-phase, laboratory-scale prototype, the absence of long-term lifetime tests, and the use of Si-based power devices. Nevertheless, the results indicate that the AC battery concept is a strong candidate for scaling to three-phase systems, EV charging infrastructure, and microgrid applications, providing an experimental proof of feasibility that can support future commercialization-oriented research.

## ACKNOWLEDGMENT

This paper is supported by the OPEVA project that has received funding within the Key Digital Technologies Joint Undertaking (KDT JU) from the European Union's Horizon Europe Programme and the National Authorities (France, Czechia, Italy, Portugal, Türkiye, Switzerland), under grant agreement 101097267. The work presented in this paper has been carried out as part of the OPEVA Demo 1 - HiL testing for integrated battery balancing and power electronics in automotive and stationary applications activities. Views and opinions expressed are however those of the author(s) only and do not necessarily reflect those of the European Union or KDT JU. Neither the European Union nor the granting authority can be held responsible for them.

Also, this study was supported by Scientific and Technological Research Council of Turkey (TUBITAK) under the Grant Number 222N269. The authors thank to TUBITAK for their supports.

## REFERENCES

- [1] Balachandran, "Battery integrated modular multilevel converter topologies for automotive applications," Ph.D. dissertation, Linköping University, Linköping, Sweden, 2023.
- [2] A. M. Rauf, M. Abdel-Monem, T. Geury, and O. Hegazy, "A review on multilevel converters for efficient integration of battery systems in stationary applications,"

- Energies, vol. 16, no. 10, p. 4133, 2023.
- [3] F. Helling, J. Glück, A. Singer, H. J. Pfisterer, and T. Weyh, "The ac battery-A novel approach for integrating batteries into ac systems," *International Journal of Electrical Power & Energy Systems*, vol. 104, pp. 150–158, 2019.
  - [4] W. Chen, B. Riar, and R. Zane, "Battery integrated modular multifunction converter for grid energy storage," in *Proc. IEEE Energy Conversion Congress and Exposition (ECCE)*, Sept. 2018, pp. 2157–2163.
  - [5] J. Rodriguez, S. Bernet, B. Wu, J. O. Pontt, and S. Kouro, "Multilevel voltage-source-converter topologies for industrial medium-voltage drives," *IEEE Transactions on Industrial Electronics*, vol. 54, no. 6, pp. 2930–2945, Dec. 2007.
  - [6] A. Ziegler, D. Oeser, B. Arndt, and A. Ackva, "Comparison of active and passive balancing by a long term test including a post-mortem analysis of all single battery cells," in *Proc. Int. IEEE Conf. and Workshop in Óbuda on Electrical and Power Engineering (CANDO-EPE)*, Nov. 2018, pp. 15–20.
  - [7] F. Helling, J. Glück, A. Singer, and T. Weyh, "Modular multilevel battery (M2B) for electric vehicles," in *Proc. 18th European Conf. on Power Electronics and Applications (EPE'16 ECCE Europe)*, Sept. 2016, pp. 1–9.
  - [8] A. M. Rauf, M. A. Monem, T. Geury, M. El Baghdadi, and O. Hegazy, "Fast active balancing system using multi-level DC converter for efficient AC-coupled battery systems in stationary applications," in *Proc. 15th Int. Conf. on Ecological Vehicles and Renewable Energies (EVER)*, Sept. 2020, pp. 1–6.
  - [9] S. Shelare, K. Aglawe, M. Dhande, S. Wagnmare, M. Giripunje, and P. Sirsat, "Battery thermal management system: A review on recent progress, challenges and limitations," in *MATEC Web of Conferences*, vol. 405, p. 02004, 2024.
  - [10] P. H. Riley, K. R. Pullen, O. Dordevic, L. DeLilo, and M. De Giorgio, "A qualitative assessment of a modified multilevel converter topology M2LeC for lightweight low-cost electric propulsion," *Engineering*, vol. 12, no. 7, pp. 496–515, 2020.
  - [11] A. Balachandran, T. Jonsson, and L. Eriksson, "DC charging capabilities of battery-integrated modular multilevel converters based on maximum tractive power," *Electricity*, vol. 4, no. 1, pp. 62–77, 2023.
  - [12] A. Kersten, M. Kuder, E. Grunditz, Z. Geng, E. Wikner, T. Thiringer, and R. Eckerle, "Inverter and battery drive cycle efficiency comparisons of CHB and MMSP traction inverters for electric vehicles," in *Proc. 21st European Conf. on Power Electronics and Applications (EPE'19 ECCE Europe)*, Sept. 2019, p. P-1.
  - [13] M. Quraan, P. Tricoli, S. D'Arco, and L. Piegari, "Efficiency assessment of modular multilevel converters for battery electric vehicles," *IEEE Transactions on Power Electronics*, vol. 32, no. 3, pp. 2041–2051, Mar. 2017.